Received April 13, 2019, accepted May 3, 2019, date of publication May 9, 2019, date of current version May 21, 2019.

Digital Object Identifier 10.1109/ACCESS.2019.2915929

CFDAMA-SRR: A MAC Protocol for Underwater Acoustic Sensor Networks

WAEL GORMA, PAUL D. MITCHELL, (Senior Member, IEEE), NILS MOROZS, (Member, IEEE), AND YURIY V. ZAKHAROV, (Senior Member, IEEE)
Department of Electronic Engineering, University of York, York YO10 5DD, U.K.

Corresponding author: Wael Gorma (wmg503@york.ac.uk)

The work of P. D. Mitchell, N. Morozs, and Y. V. Zakharov was supported in part by the U.K. Engineering and Physical Sciences Research Council (EPSRC) under Grant EP/P017975/1 and Grant EP/R003297/1.

ABSTRACT Underwater acoustic sensor networks are an enabling technology for many applications. Long propagation delays and limited bandwidth of the acoustic channel place constraints on the trade-off between achievable end-to-end delay, channel utilization, and fairness. This paper provides new insights into the use of the combined free/demand assignment multiple access (CFDAMA) schemes. The CFDAMA can be classified as adaptive TDMA, where capacity is usually assigned on demand. The CFDAMA with round robin requests (CFDAMA-RRs) are shown to minimize end-to-end delay and maximize channel utilization underwater. It sustains fairness between nodes with minimum overhead and adapts to changes in the underwater channel and time-varying traffic requirements. However, its performance is heavily dependent on the network size. The major contribution of this paper is a new scheme employing the round robin request strategy in a systematic manner (CFDAMA-SRR). Comprehensive event-driven Riverbed simulations of a network deployed on the sea bed show that the CFDAMA-SRR outperforms its underlying scheme, CFDAMA-RR, especially when sensor nodes are widely spread. Considering node locations, the novel scheme has a bias against long delay demand assigned slots to enhance the performance of the CFDAMA-RR. The illustrative examples show good agreement between the analytical and simulation results.

INDEX TERMS CFDAMA, medium access control, TDMA, underwater acoustic sensor networks.

I. INTRODUCTION

Underwater Acoustic Sensor Networks (UASNs) are an enabling technology for numerous underwater scientific, industrial and homeland security applications [1]. The use of acoustic waves underwater places constraints on the functionality of Medium Access Control (MAC) protocols. Long propagation delays and limited distance-dependent bandwidth are key constraints, which pose challenges to the design of MAC protocols including attempts to strike a balance between network end-to-end delay and throughput [2]. Low-cost sensing and communication devices are now being developed, which will make the deployment of many underwater sensor nodes (as many as 100 nodes or more) feasible in the future [3]. Due to the special characteristics of the underwater environment, specially designed underwater MAC protocols are very much in demand.

The associate editor coordinating the review of this manuscript and approving it for publication was Fang Yang.

Contention-based MAC protocols can be less efficient for centralized topologies due to the potential high contention in winning the channel [4]. However, they are more practical for small distributed networks. Carrier Sense Multiple Access (CSMA) schemes require substantial guard intervals to accurately sense the acoustic channel, leading to poor delay/utilization performance [5]. Time Division Multiple Access (TDMA) [6] is a promising baseline for underwater MAC protocols. It enables allocation of variable data rates by just changing the number of time slots allocated to each node [5]. Scheduling is the main challenge facing TDMA-based MAC protocols underwater. Propagation delays typically need to be estimated in order to maintain synchronization between nodes. The estimation of long and time-variant propagation delays can be dealt with using handshaking. [7] proposed a centralized protocol named Transmit Delay Allocation MAC (TDA-MAC) for single-hop UASNs composed of sensor nodes connected to the same gateway. It is shown to provide high throughput performance, without

global clock synchronization but rather a handshaking technique to estimate delays and attain packet arrivals without collisions. The most practical network type suiting TDMA-based protocols is the centralized type. The problem of scheduling has also been addressed in [8]. The authors called their protocol the staggered TDMA underwater MAC protocol (STUMP). It is a collision-free MAC protocol exploiting node location diversity and alleviating the impact of slow propagation speed. The protocol leverages propagation delay information to increase channel utilization by allowing concurrent data transmissions from several nodes.

Schedule-based techniques can also be combined with contention-based schemes [4]. This combination is classified as Adaptive TDMA where capacity is usually assigned on demand. Three capacity assignment schemes have been examined in [2]. Demand assignment, Free assignment and the Combined Free and Demand Assignment Multiple Access (CFDAMA) schemes. Free assignment is shown to offer close to the theoretical minimum end-to-end delay, but only at low channel loads. Demand assignment can support much higher channel loads, but with longer delays. CFDAMA is capable of minimizing the end-to-end delay and maximizing the channel utilization. It has been proposed in [9] for satellite channels to enhance the delay/utilization performance of long delay geostationary satellite links. It is capable of improving the overall performance of networks which suffer from long propagation delays and limited capacity such as UASNs. The presence of the free assignment strategy in CFDAMA works as a backup slot provider. It means that CFDAMA can adapt to the severe underwater conditions that may bring about instantaneous connection loss, preventing sensor nodes from sending requests. Combining two different MAC schemes with the possibility of using several request strategies gives CFDAMA the flexibility to meet different network requirements and applications. Simplicity is a fundamental feature of CFDAMA as most of the processing is done at a master node, typically equipped with a terrestrial high-speed link, synchronized clock and a more sustainable power source.

When designing and evaluating the performance of MAC protocols, applications associated with environmental monitoring are usually characterized with periodic data traffic models [7]. On the other hand, the Poisson traffic model, which enables tractable theoretical analysis, is a more accurate representation for other applications [10]–[12], such as remote fish detection or security monitoring. This paper evaluates the performance of CFDAMA schemes underwater with two distinct traffic types based on a Poisson model and a self-similar model [13]. As CFDAMA is a combined protocol, it is tolerant to changes in the type of data traffic.

In [2], in which we first considered CFDAMA for UASNs, the study is limited to a conventional request strategy based on random access. The impact of different request strategies has not been examined. Following that, we introduced a new CFDAMA scheme in [14], called CFDAMA with Intermediate Scheduler, to significantly reduce the average round-trip time required for making capacity requests and receiving subsequent acknowledgements. This enhances the overall delay/utilization performance of CFDAMA. There, the analysis of delay performance focuses on the dominant factors determining the average end-to-end delay of packets. Queuing time at sensor nodes has not been covered. Spatial distribution of nodes and the statistical behavior of traffic sources have not been investigated. Due to the long propagation delay underwater and the fact that sensor nodes can be widely spread, implementing CFDAMA with one of the conventional request strategies and without considering the location of nodes results in poorer efficiency than the level of which the scheme is capable. Beyond the previous work, we introduce in this paper a new scheme, CFDAMA with Systematic Round Robin requests (CFDAMA-SRR), to boost the effectiveness of CFDAMA underwater. The key contributions in this paper include:

- A new CFDAMA scheme, i.e. CFDAMA-SRR.
- Analysis of CFDAMA-SRR behavior for representative underwater scenarios, through analytical and numerical simulations.
- Recommendations on the trade-off between CFDAMA-SRR parameters under two distinct traffic conditions.
- Comprehensive simulation results based on a realistic underwater sensor deployment for seismic monitoring in oil reservoirs, with the use of the BELLHOP acoustic field computation program [15].
- Evaluation of CFDAMA-SRR performance via an acoustic channel simulated based on well-known underwater propagation and ambient noise models.

The rest of the paper is organized as follows: Section II introduces CFDAMA, Section III describes the new CFDAMA variant, Section IV presents the simulated underwater scenarios and parameters, Section V illustrates the outcomes of the detailed simulation study, and finally, Section VI concludes the paper.

II. THE CFDAMA PROTOCOL

This section outlines the operation of CFDAMA, and describes the CFDAMA scheduling algorithm and frame structures. This is required in order to understand the new scheme proposed in the next section as well as some related mathematical analysis and comparative performance results presented later.

Detailed discussion on CFDAMA can be found in [2], [16], [17]. CFDAMA combines two capacity assignment strategies: free assignment and demand assignment. The major advantage of the CFDAMA protocol is that it exploits the effectiveness of demand assignment in achieving high channel utilization and the contention-less nature of free assignment with a minimum end-to-end delay close to the minimum bound of a 0.5 gateway hop. A gateway hop relates to a transmission from a sensor node to the gateway and back down to the sensor nodes again, equivalent to one round trip as shown in Fig. 1.

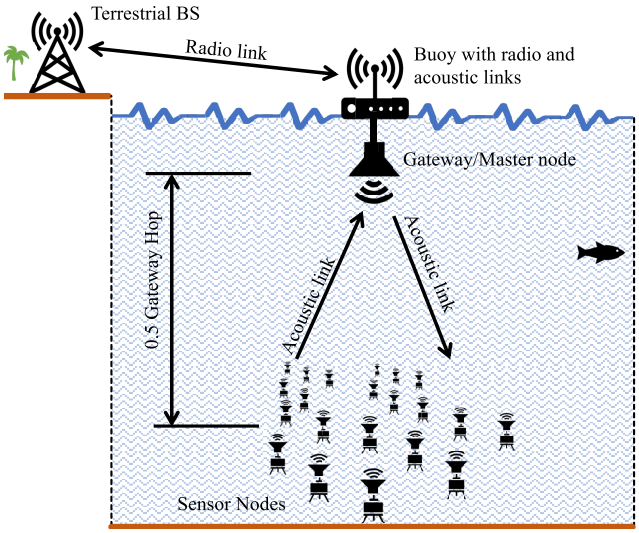

FIGURE 1. An example of centralized UASN.

A. CFDAMA SCHEDULING ALGORITHM

Due to the time and space uncertainty of the underwater environment, many applications require a form of global scheduling as for instance used in [7], [8], [10]. Fig. 1 illustrates an example of a centralized UASN. The node near the sea surface is called master node or gateway and should incorporate a high-speed connection to the terrestrial world. Nodes that are deployed at greater depths are the sensor nodes. CFDAMA scheduling is performed using two serving tables operating at the gateway. They are known as the free assignment table and the reservation request table. The cycle starts when a request is made. Allocation of both types of slots (free and demand) is done on a frame-by-frame basis. The global scheduler informs all sensor nodes of their allocations in a Time Division Multiplex (TDM) fashion on the forward frame. Slots are initially assigned using the demand assigned mode, according to the entries in the reservation request table. Once all requests waiting in the queue have been dealt with, the scheduler then switches to free assignment mode and starts to freely assign slots to the remaining nodes in a round robin fashion. This is made by assigning individual free assigned slots, one after another, to the nodes whose IDs are, at that moment, waiting at the top of the free assignment table. Following each slot allocation, each served node-ID is dropped to the bottom of the table. This approach maintains fairness between nodes. Likewise, each time a node is allocated a set of successive demand assigned slots based on the number requested, its ID is also moved to the tail of the free assignment table.

B. CFDAMA FRAME STRUCTURES

To implement CFDAMA, two frame structures are needed, i.e. forward frame (from the gateway to the sensor nodes) and return frame (from the sensor nodes to the gateway). Both frames are made up of two segments: a data slot segment plus a segment of request slots in the case of the return frame.

Algorithm 1 CFDAMA Algorithm Implemented at the Gateway, N_{RS} = Number of Requested Slots by a Node, Tab_1 = the Free Assignment Table, Tab_2 = the Reservation Request Table, F = Free Slot, D = Demand Slot, j = Pointer

```
for every return frame do
    update Tab2 based on new requests arrived during return frame(j)
    while available slots in forward frame (j) ≠ 0 do
        if Tab2 is not empty then
            in forward frame (j) assign N_RS D slots to 1st node in Tab2
            remove this entry id from Tab2
            move this entry id to tail of Tab1
        else
            assign 1 F slot to the node whose id is at the top of Tab1
            move this entry to tail of Tab1
        end if
    end while
end for
```

Whereas, in the case of the forward frame, they are a segment of acknowledgement slots plus an optional data slot segment (if required [14]). Data slots are allocated to nodes either as free assigned slots (F) or demand assigned slots (D). Request packets are transmitted in the request slots on the return frame, and are subsequently acknowledged in the acknowledgement slots of the forward frame. The forward frame is delayed with respect to the return frame by a period long enough to allow the request packets that are received in the return frame to be immediately processed and acknowledged with assignments in the following forward frame. Request slots can be accessed using different strategies based on the CFDAMA variant used, for example, a round robin strategy for the CFDAMA-RR scheme [18]. The exact frame formats depend on which CFDAMA variant used.

Fig. 2 illustrates an arbitrary transmission cycle in a randomly selected j^{th}return frame of CFDAMA-RR. In this example, based on round robin turns on a frame-by-frame basis, the turn at this instant is for the n^{th}, $(n+1)^{th}$ and $(n+2)^{th}$ nodes to make requests. As the figure shows, CFDAMA-RR devotes a region located at the start of the return frame to round robin request slots. In this instance, the sensor node can make a request, if required, and the number of slots to be requested by a node is given by:

$$N_{RS} = N_{PQ} - N_{OR} \tag{1}$$

where N_{RS} is the number of requested slots, N_{PQ} is the number of queued packets and N_{OR} is the number of outstanding requests. The illustrated example also shows that these nodes are transmitting data packets according to allocated D and F slots acknowledged in the $(j-1)^{th}$ forward frame. Algorithms 1 and 2 outline the implementation of this CFDAMA-RR cycle. Furthermore, with reference to Fig. 2, each node is responsible for aligning the arrival of its packet

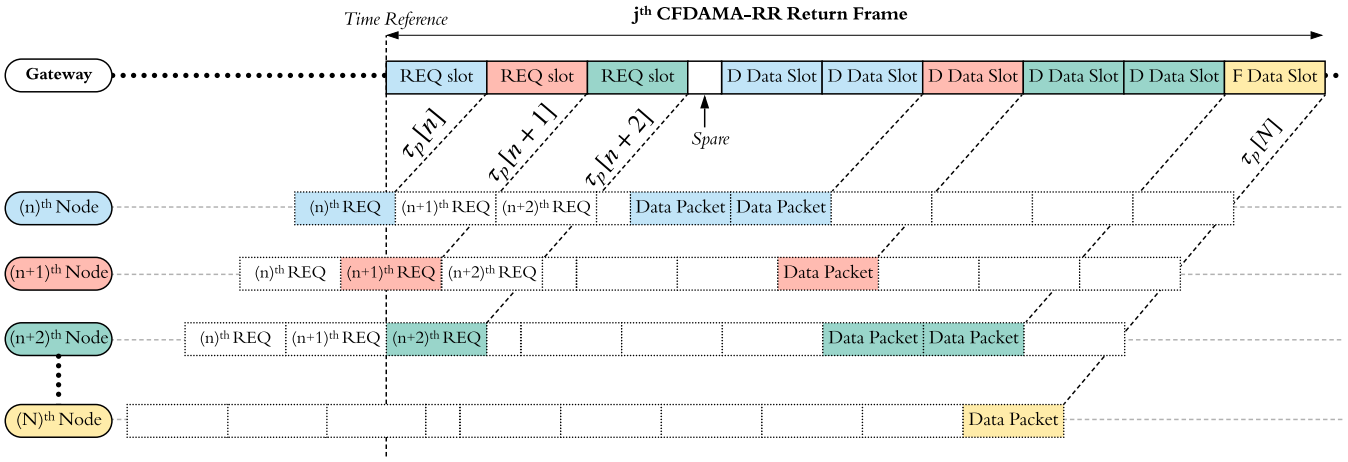

FIGURE 2. An arbitrary CFDAMA-RR return frame with some allocations.

Algorithm 2 CFDAMA Algorithm Implemented at Each Sensor Node, N_{PQ} = Number of Packets Queued, N_{OR} = Number of Outstanding Requests, N_{GS} = Number of Granted Data Slots

```
for every forward frame do
    if (N_GS ≠ 0) in forward frame(j) then
        read due time of granted slots
        schedule N_GS transmissions as appropriate
    end if
    if a request slot is due in return frame (j + 1) then
        count N_PQ and N_OR
        N_RS = N_PQ − N_OR
        make a request of N_RS slots in return frame(j + 1)
    end if
end for
```

with the beginning of its allocated slot referenced at the gateway by transmitting the packet $\tau_p[n]$ seconds prior to the due time of the allocated slot. $\tau_p[n]$ is the propagation delay between the n^{th} sensor node and the gateway. For practical synchronization guard intervals can also be added as appropriate in case of node clock/location drift. Nodes must synchronize their built-in clocks with the master node's clock. In practice, propagation delays need to be estimated in order to attain this synchronization. Typically, this estimation of the long and time-variant propagation delay of acoustic waves is dealt with using a handshake technique [7] as often as required. Spare capacity is inserted in both frames to make their lengths equal for simplicity.

III. CFDAMA WITH SYSTEMATIC ROUND ROBIN REQUESTS (CFDAMA-SRR)

CFDAMA with Round Robin requests (CFDAMA-RR) was originally designed to get around the limitations of the Random Access (RA), Packet Accompanied (PA) and Combined Request (CR) request strategies [16], [17], and to maintain unbiased access rights for all nodes. This section introduces our new CFDAMA variant, CFDAMA-SRR, which has CFDAMA-RR as its underlying strategy.

A. CFDAMA WITH ROUND ROBIN REQUESTS (CFDAMA-RR)

To maintain fairness between nodes in accessing the channel, the CFDAMA-RR scheme eliminates the possibility of losing the channel due to contention between nodes or channel domination by transmitting nodes [18]. CFDAMA-RR uses the round robin technique to assign request slots to individual nodes. Therefore, nodes are not inhibited by other nodes from making requests, which means the scheme is contention less.

1) DRAWBACKS OF CFDAMA-RR

Under certain conditions, CFDAMA-RR may have drawbacks some of which are summarized as follows:

- Its delay performance is heavily dependent on the number of nodes; gaining access to the channel becomes less regular as the number of nodes increases.
- The likelihood of wasting free assigned slots granted to nodes that have no data to send at the instance of a free slot arrival. This is not specific to CFDAMA-RR, but it is most likely to happen with it.
- Its delay performance also relies on the number of request slots per frame. A large number of request slots can lead to unreasonably high overhead and low throughput performance.

B. CFDAMA WITH SYSTEMATIC ROUND ROBIN REQUESTS (CFDAMA-SRR)

For the sake of improving the performance of CFDAMA-RR [18], the correlation between the round-trip delay τ_r and the type of granted transmission slot needs investigating. Each successfully received packet must have gone through one of three possible scenarios:

- Scenario 1: in which the packet gets through by the use of a free assigned slot.

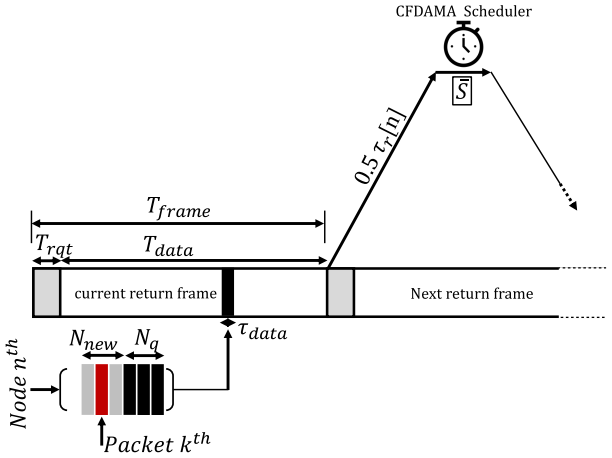

FIGURE 3. Systematic Round Robin Timing.

- Scenario 2: in which the packet gets through by the use of an undue reserved slot, i.e. a slot requested for a preceding packet from the same node.
- Scenario 3: in which the packet gets through by the use of a due reserved slot, i.e. its own requested slot.

With reference to Fig. 3, and by considering an arbitrary n^{th} node and the case where there are N_{new} new packet arrivals in the current CFDAMA frame, we will find the expectation through which scenario the arbitrary k^{th} packet will be transmitted. For simplicity the data slot duration τ_{data} is used as a time unit in the following discussion. Each particular node can have one request slot per a CFDAMA frame. The duration of CFDAMA frame is denoted by T_{frame} and is given by:

$$T_{\text{frame}} = T_{\text{data}} + T_{\text{rqt}} \tag{2}$$

where T_{rqt} is the total duration of request slots in the frame and T_{data} is the total duration of data slots in the frame. When $T_{\text{data}} \gg T_{\text{rqt}}$, which is usually the case for low frame overheads, then $T_{\text{frame}} \approx T_{\text{data}}$. In every CFDAMA frame, there will be two possibilities of the k^{th} packet arrival: arriving within the round-trip delay denoted by $\tau_r[n]$ time slots or arriving after it. We will assume that on average the N_{new} new packet arrivals happen uniformly within a CFDAMA frame, which contains T_{frame} time-slots, and thus, the expected number of new packets within $\tau_r[n]$ is given by:

$$x = \left\lceil \frac{N_{\text{new}}\tau_r[n]}{T_{\text{frame}}} \right\rceil \tag{3}$$

Therefore, if $1 < k < x$, called constraint C_1 in the following discussion, then the three packet escaping scenarios (defined above) could be possible. However, if $x < k < N_{\text{new}}$, called constraint C_2 in the following discussion, then Scenario 2 will be impossible as there will be no undue requested slots left. If C_2 is satisfied, the tagged packet arrives after $\tau_r[n]$ time-slots, and thus, will have to be granted either a free assigned slot (Scenario 1) which also must occur after $\tau_r[n]$ time-slots or wait for its own requested slot (Scenario 3).

It is sensible to assume that the only way that the k^{th} packet escapes is via Scenario 3 when k exceeds a certain threshold. At high offered traffic levels, there must be a number of old packets N_q from previous CFDAMA frame(s) waiting in the node's queue ($N_q > 0$). Thus, the certain threshold is $(a+b)$, which is the maximum total number of free-assigned slots granted to the n^{th} node during the interval of $(\tau_r[n] + T_{\text{frame}} + \bar{S})$, where b represents the maximum number of free-assigned slots granted to a node during the interval of $\tau_r[n]$ time-slots, and for N number of nodes, it is given by:

$$b = \left\lceil \frac{\tau_r[n]}{N} \right\rceil \tag{4}$$

a represents the maximum number of free-assigned slots in a CFDAMA frame. In other words, the approximation can be made here is that if $N_q + k > a$, called constraint C_3 in the following discussion, the only way the k^{th} packet escapes is through its due demand requested slot (Scenario 3). Assuming $k\Delta$ is the expected instant of arrival of the k^{th} packet, the packet needs to wait for $(\tau_r[n] + T_{\text{frame}} + \bar{S} - k\Delta)$ slots in order to be granted its own demand-assignment slot. Since $\tau_r[n]$ is typically large underwater, $\bar{S}$ is insignificant compared to τ_r, on average the expected instant of the packet arrival $k\Delta$ can be close to $T_{\text{frame}}/2$, and T_{frame} is comparable to τ_r, this waiting interval can be approximated to $\gamma\tau_r[n]$, where $\gamma \approx 1.5$ is a constant.

During the interval $\gamma\tau_r[n]$, there are: $\lceil \gamma\tau_r[n]/N(1-d) \rceil$ free-assigned slots available for the tagged n^{th} node, where $(1-d)$ is the fraction of free-assigned slots in a CFDAMA frame. This indicates that there will be a relatively large number of free-assignment slots available to use and that the number increases with $\tau_r[n]$. The assumption that ought to be made now is that if $[(N_q + k) < \lceil \gamma\tau_r[n]/N(1-d) \rceil]$, called constraint C_4 in the following discussion, then the k^{th} packet will certainly escape through a free-assigned slot (Scenario 1). This event occurs more frequently when $\tau_r[n]$ is large because the fraction of demand-assigned slots (d) in a CFDAMA frame is also reduced. Subsequently, the k^{th} packet will also have more opportunities to escape using an undue requested slot (Scenario 2).

TABLE 1. List of constraints.

Denotation	Constraint	Available Scenarios
C_1	$1 < k < x$	Scenarios 1, 2, or 3
C_2	$x < k < N_{\text{new}}$	Scenarios 1 or 3
C_3	$N_q + k > a$	Scenario 3
C_4	$N_q + k < \lceil \gamma\tau_r[n]/N(1-d) \rceil$	Scenario 1

Considering Equations (3) and (4) and constraints (C_1, C_2, C_3 and C_4) summarized in Table 1, the round-trip delay $\tau_r[n]$ has a significant impact on determining the scenario through which a packet will be transmitted. More specificity, $\tau_r[n]$ will affect the transition from free assignment to demand assignment, and hence, the delay/utilization performance. This transition will also depend on the position of the new packet in the node's queue with respect to the interval $\tau_r[n]$.

Due to long propagation delays and sensor nodes that are typically located at different distances from the central gateway, implementing the CFDAMA-RR strategy without a form of location-based arrangement will cause the scheme to miss an opportunity of even better performance. For the reader's reference, Table 3 lists the mathematical terms used in this section.

1) CFDAMA-SRR SOLUTION

Satisfying the constraint C_4 will depend not only on τ_r but also on the value of the offered traffic and the statistical behavior of data traffic. They will be instantaneously determining the term $(k + N_q)$ in the constraint C_4. Satisfying constraint C_4 means plenty of free assigned slots will be available. Nodes that are located farther away from the gateway will allow their new packets to have a higher chance to satisfy the constraint C_4 than the nodes that are located closer. The closer nodes will actually have a higher chance that their newly arrived packets will satisfy the constraint C_3, and hence, have to wait for at least the period of τ_r to obtain a slot. If C_3 is satisfied and there are not enough request slots in the frame, newly arriving packets will have to wait for multiple frames before a capacity request can be made for them.

Given the above, this paper introduces a new variant of CFDAMA-RR, namely CFDAMA-SRR. The new scheme works the same way as CFDAMA-RR does, described in Section II, except for the fact that the round robin algorithm works with respect to the location of sensor nodes. The nodes make their capacity requests not only in a round robin fashion but also in a location-based manner with respect to the location of their centralized scheduling node. Opportunities to make a request are given successively to adjacent nodes one after another, starting from the center to the edge of the network. CFDAMA-SRR can reduce the possibility that C_3 is satisfied and boost the possibility that C_4 is satisfied. At high channel loads, this new scheme can maximize the use of each single request opportunity leading to enhanced delay/utilization performance. When a node makes a single request for more than one slot, a run of successive slots is then allocated allowing back to back packet transmissions. Subsequently, the end-to-end delay of back to back packet transmissions is determined by the inter-arrival time of packet generations with respect to the data slot duration. CFDAMA-SRR systematizes the distribution of request opportunities which works in favor of the utilization of a single request rather than multiple requests for the same demand. It also allows more time for those nodes located further away from the gateway to maximize the use of an increased number of free assigned slots owing to their longer round trips.

C. CFDAMA-SRR DELAY ANALYSIS

In order to gain useful insights, this section provides an analytical approach to evaluating the average end-to-end delay performance of CFDAMA-SRR. This approach follows similar steps to the derivation used in [19] to model the performance of a CFDAMA variant of a small number of terminals for satellite systems. However, the assumptions made for underwater scenarios are different. Packets make Bernoulli attempts continually until they get through either as Scenario 1, Scenario 2 or Scenario 3 described in Subsection (B). The average end-to-end delay of packets will depend on the scenario it goes through. The analytical approach here is to evaluate the average delay a tagged k^{th} packet would experience based on the probability of each of the three scenarios.

In UASNs the packets end-to-end delay is heavily dominated by both the propagation delay and the number of sensor nodes in the network. Therefore, the claim this section will fulfill is that the CFDAMA average waiting and service time can be modeled as a $M/G/1$ queue when the round-trip delays are long. Packet transmissions will be dominated by Scenario 1 and the round robin free assignment scheme will be in operation most of the time when the round-trip delays are long. The following analysis steps will lead to obtaining the approximated mean and variance values of the waiting and service time. Plugging in these values in the Pollaczek-Khinchin formula [20] of the $M/G/1$ queue will result the total waiting and service time. Finally, the average end-to-end delay of packets can be calculated using this waiting and service time plus the average propagation delay. With respect to the CFDAMA-SRR frame illustrated in Fig. 3, the frame has T_{frame} timeslots where T_{frame} is proportional to the total number of sensor nodes N. The frame size and data slot size can be chosen based on the desired throughput and transmission rate in a given underwater scenario. For convenience in the following discussion, the time-slot duration τ_{data} is used as the time unit. For example, the round-trip delay is denoted by τ_r time-slots. For a Poisson data traffic source, the probability that N_{new} new packets arrive in a CFDAMA frame is given by [19]:

$$P_r\{N_{\text{new}}\} = \frac{e^{-\lambda T_{\text{frame}}} \lambda^{N_{\text{new}}}}{N_{\text{new}}!} \tag{5}$$

where $\lambda = \Lambda/N$ is the arrival rate per time slot at each node. Λ is the network packets arrival rate per time slot. The beginning of the CFDAMA frame is defined to be the time origin. If a node's queue (at this instance) is not empty, it can send a request to the CFDAMA scheduler at the beginning of the next frame. The expected instant of arrival of the first due demand-assigned slot(s) is:

$$Y = \tau_r[n] + \bar{S} + T_{\text{frame}} \tag{6}$$

where $\bar{S}$ is queuing delay in the demand-assignment table of the scheduler, to be addressed later. The average period between two successive free assigned slots to a particular node is $N/(1 - d)$, where $(1 - d)$ is the fraction of free assigned slots in a CFDAMA frame (table 2 summarizes mathematical terms). Provided that the free-assignment strategy is round robin. Therefore, the probability that a packet at

TABLE 2. List of mathematical terms.

Term	Description
N	Number of nodes
T_{frame}	CFDAMA frame duration
T_{data}	Total data slots duration in a frame
T_{rqt}	Total request slots duration in a frame
τ_{data}	data slot duration
τ_{rqt}	data slot duration
$\tau_{\text{r}}[n]$	Round-trip delay of n^{th} node
$\tau_{\text{p}}[n]$	propagation delay between n^{th} node and gateway
N_{q}	Number of old packets
k	Packet's order in node's queue
n	Node's pointer
N_{new}	Number of newly arrived packets
x	Random variable = number of new packets in τ_{r}
a	Number of free slots in CFDAMA frame
b	Number of free slots during τ_{r}
d	Fraction of demand assignment in CFDAMA frame
γ	Constant
λ	Packet arrival rate per nodes
Λ	System packet arrival rate
$E(Q)$	Expected queueing delay
η	A ratio N/τ_{r}
$\bar{T}$	Waiting and service time
$\bar{T}_{\text{r}}$	Average propagation delay
$\bar{D}$	Overall CFDAMA mean delay

the front of the node's queue escapes by a free assigned slot (scenario 1) is:

$$p = \begin{cases} (1-d)/N & non-empty\ queue \\ 2(1-d)/N & empty\ queue \end{cases} \tag{7}$$

By considering an arbitrary k^{th} packet of the N_{new} new arriving packets at a tagged randomn^{th} node in the current CFDAMA frame, one of two potential cases the arriving packet will go through, defined as follows:

- when the node queue is empty, i.e. $N_{\text{q}} = 0$
- when there are old packets queued up, i.e. $N_{\text{q}} > 0$

In the underwater scenarios some assumptions can be made, as shown later, which means precise calculation of these probabilities is not required in this discussion. The scheduler queue delay $\bar{S}$ is generally negligible compared with the round-trip delay. Thus, the general unconditional mean queuing delay is:

$$E(D) = \sum_{N_{\text{q}}=0}^{T_{\text{frame}}} P_{N_{\text{q}}} E(D|N_{\text{q}}) \tag{8}$$

The computations of the k^{th} packet delay using Equation (8) become tedious as k increases. To reduce the computational complexity, some of the constraints from the discussion of Section III-B can be used. If the constraint C_3 $(N_{\text{q}}+k > a)$ is satisfied, then the only way the packet escapes is via its due demand assigned slot (Scenario 3). The expected end-to-end delay in this case will be equivalent to demand-assignment theoretical delay and given by the following:

$$E(D_{\text{k}}|N_{\text{new}}, N_{\text{q}}, N_{\text{q}}+k>a) = T_{\text{frame}} + \tau_{\text{r}}[n] + \bar{S} - k\Delta \tag{9}$$

As described in subsection III-B, during this waiting interval there are $[\gamma\tau_{\text{r}}[n]/N(1-d)]$ free-assigned slots available for the tagged n^{th} node. This shows that the number of free-assignment slots will depend on τ_{r} and N. To reflect on the effect of both the long round-trip delays and number of UASNs nodes on the performance of CFDAMA-SRR underwater, a normalization parameter is introduced to the analysis. It is denoted by η and defined as the ratio between the two parameters $N\tau_{\text{slot}}/\tau_{\text{r}}$, i.e. $\eta = N\tau_{\text{slot}}/\tau_{\text{r}}$. By plugging η in the former expression ($[\gamma\tau_{\text{r}}/N(1-d)]$), the number of available free-assignment slots will be $[\gamma(1-d)/\eta]$. As η decreases, the benefits of free-assignment slots are increased. With respect to the constraint C_2 and C_4 from the previous section, if $x < k < N_{\text{new}}$, then Scenario 2 will be impossible as the tagged packet cannot be transmitted via an undue requested slot, and if $[(N_{\text{q}}+k) < [\gamma(1-d)/\eta]]$ then the k^{th} packet will certainly escape through a free-assigned slot (Scenario 1). These two constraints will be satisfied more frequently when $\eta \ll 1$ $(i.e.\tau_{\text{r}} \gg N\tau_{\text{slot}})$. Therefore, the average service time that the k^{th} packet will take when it reaches the head of the node's queue will rely mainly on Scenarios (1 and 3) and can be expressed as :

$$E(Q) \approx \sum_{i=1}^{\Omega} p(1-p)^{i-N_{\text{new}}} i + [1 - \sum_{i=1}^{\Omega} p(1-p)^{i-N_{\text{new}}}][\Omega] \tag{10}$$

The first term in (10) represents the delay of the k^{th} packet when transmitted as Scenario 1 and the second term gives the delay of the k^{th} packet when transmitted as Scenario 3, and p is given by expression (8). The Equation (10) can be simplified to:

$$E(Q) = \frac{[1-(1-p)^{\Omega+1}]}{p} - (\Omega+1)(1-p)^{\Omega} + \Omega(1-p)^{\Omega} \tag{11}$$

where Ω is a constant given by:

$$\Omega = \lceil \gamma\tau_{\text{r}} \rceil, \text{ and } p = \frac{1-d}{N} = \frac{(1-d)\gamma}{\eta\Omega}$$

For $(\Omega \gg 1)$, as it is typically the case with underwater scenarios due to the large τ_{r}, E(Q) can be simplified to:

$$E(Q) \approx \frac{(1-e^{-\nu})}{p} \tag{12}$$

where $\nu = (1-d)\gamma/\eta$. This simplification is based on the relation $e^{-\nu} \approx (1-(\nu/\Omega))^{\Omega}$. For small values of η, d will be small, and as a result, the ν value will be reactively large. Thus, $e^{-\nu} \ll 1$. For example when η and $d < 0.1$, $e^{-\nu}$ will be less than $1.4\,x10^{-6}$ which is negligible. This suggests that for a small η, i.e. long round-trip delays τ_{r}, the average service time of a packet at the head of the node's queue is approximated as:

$$E(Q) = \frac{1}{p} = \frac{N}{(1-d)} \approx N \quad for\ d \ll 1 \tag{13}$$

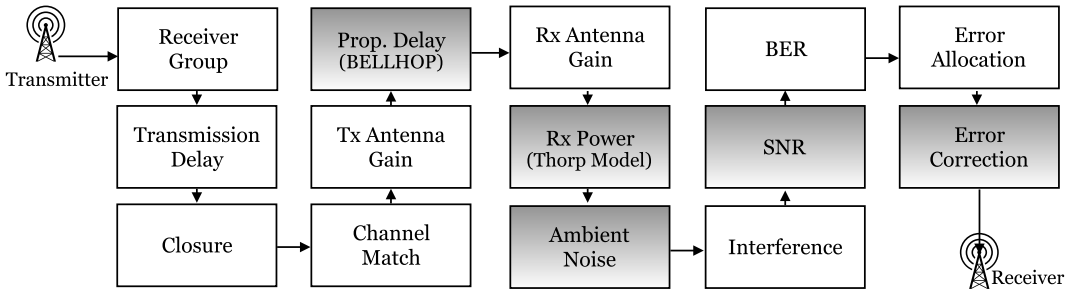

FIGURE 4. Underwater Acoustic Network Channel in Riverbed Modeler [14].

Hence, the mean value and the variance of the service time are N and $N(N-1)$ in respectively. Plugging in the mean and variant values in the Pollaczek-Khinchin formula will result in the total waiting and service time as follows:

$$\bar{T} = N + \frac{\lambda N(N-1)}{2(1-\lambda N)} \tag{14}$$

where λ is the arrival rate per node in packets/slot, i.e. equivalent to Erlangs [21]. The average packet end-to-end delay can then be given by:

$$\bar{D} = \bar{T} + \bar{T}_{\mathrm{r}} \tag{15}$$

where $\bar{T}_{\mathrm{r}}$ is the packets average propagating delay of N nodes and can be obtained from:

$$\bar{T}_{\mathrm{r}} = \sum_{n=1}^{N} \frac{\gamma \tau_{\mathrm{r}}[n]}{N} \tag{16}$$

Fig. 7, Fig. 8 and Fig. 9 illustrate a good agreement between the simulation and analytical results using Equation (15). The results have been obtained for various underwater scenarios and CFDAMA parameters which are detailed in Section IV.

IV. SIMULATION SET-UP AND DISCUSSION

Riverbed Modeler (RM) [22] has been used to develop a simulator of the underwater scenarios described in this section. To reflect on the propagation of acoustic waves underwater, RM follows the stages shown in Fig. 4. This section provides the details.

A. SPEED OF SOUND UNDERWATER

The speed of sound through water is a fundamental property of acoustic communication channels and is the dominant bottleneck of the overall network performance. The sound speed is a function of a number of underwater environmental parameters e.g. the temperature, pressure and salinity of the water, and hence, it is variable in space and time [23]. The propagation speed of sound underwater near the surface gradually decreases because the temperature decreases rapidly but the pressure remains more or less the same. After that, it reaches a point where it is minimal after which the temperature stays constant but the pressure increases causing the sound speed to increase very slowly. This means sound signals (rays) will

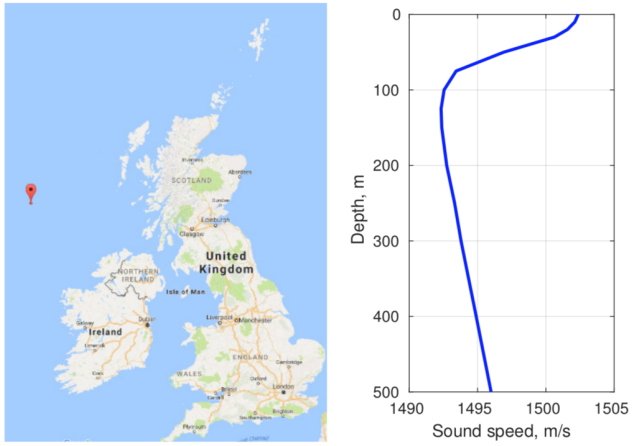

(a) (b)

FIGURE 5. Example of an SSP in the North Atlantic Ocean [7]. (a) Google maps location. (b) Sound speed profile.

follow curved paths which will be different to the Euclidean distances. For a realistic Sound Speed Profile (SSP) as used in [7], Fig. 5 depicts a case derived by Dushaw [24] from the 2009 World Ocean Atlas temperature, pressure and salinity data at $(56.5^{o}N, 11.5^{o}W)$ in April, i.e. around the North Atlantic Ocean off the coast of the UK and Ireland. The SSP caused refraction of the propagated acoustic rays, which in turn results in curved trajectories. These trajectory traces have been extracted using the BELLHOP ray tracing program [25] and accurate propagation delays have been obtained.

B. UNDERWATER ACOUSTIC CHANNEL MODEL

A vector containing the actual values of node-to-node propagation delays based on the SSP depicted in Fig. 5 have been extracted from BELLHOP and imported into RM. An empirical model [26] is used to predict the underwater ambient noise based on channel bandwidth given in table 3. The Thorp model [27] is used to calculate the absorption coefficient in order to be used to estimate the received power. Based on these parameters, the signal to noise ratio (SNR) experienced by each transmitted packet is evaluated, and subsequently, the Bit Error Rate (BER) is estimated to determine the packet's eligibility for successful reception at its receiver. This BER is not the empirical rate of bit errors,

but rather the expected rate based on a look-up table and the corresponding SNR value. The RM counts the number of bit errors in each packet and maintains a bit-error accumulator. The acceptability test of a packet at the receiver is based on both the interference between packets as well as the proportion of bit errors due to noise. If a non-zero-length packet overlap between successive packet arrivals is detected, the receiver rejects all packets involved in the overlap. If the number of bit errors in a packet exceeds a certain threshold, the receiver rejects the packet.

C. DATA TRAFFIC CHARACTERISTICS

Poisson data traffic is a traditional traffic model that has been for decades the first choice for evaluating communication protocol performance. The main feature of this model is that the inter-arrival times between packets can be modeled as independent exponentially distributed random events at each source. In spite of some arguments made in a number of studies claiming that the Poisson model is not suitable for many applications, e.g. [28], [29], it is still widely used for simulation-based studies as a tool allowing comparison with relatively tractable theoretical analysis. This applies also to UASNs, e.g. [10]–[12]. Many UASN applications can be characterized by periodic data traffic models, particularly for applications associated with environmental monitoring tasks [7]. In such tasks, the network is configured in a way that every node transmits a packet periodically containing a sensor reading to a base station or a gateway node, e.g. [30]. In [13], it is found that statistics of data traffic generated by event-based wireless sensor applications are found to obey the Pareto ON/OFF distribution very well. Two distinct traffic models (Poisson OFF and Pareto ON/OFF) have been developed in RM for the evaluation of CFDAMA-SRR performance in this paper.

D. NETWORK TOPOLOGY AND SIMULATION PARAMETERS

With reference to Fig. 1, different scenarios of 3 different network sizes (20, 50 and 100 nodes) and several packet durations have been studied. Sensor nodes are distributed randomly across a coverage area of 6×6 km, using the RM simulator with a centralized gateway at a 20m depth just above the central point of the coverage area. The depths of sensor nodes obey a uniform random distribution and are located between 470 and 490 m. The selection of these parameters corresponds to a typical oil reservoir seismic monitoring scenario, e.g. [31]. They have been chosen to be within the range of operating parameters of current commercial modems. For example, but not limited to, the EvoLogics S2CR 15/27 modem [32]. The trade-off between CFDAMA parameters has been assessed. These scenarios can provide a range of different test options for performance evaluation of the CFDAMA schemes or comparison with other approaches in the literature. The simulation parameters are listed in Table 3. Using given data slot duration (τ_{data}), request slot duration (τ_{rqt}), number of data slots (N_{ds}) and number of request slots (N_{rs}), one can obtain T_{frame} from Equation (2), which can be rewritten with respect to the aforementioned parameters as follows:

$$T_{\text{frame}} = N_{\text{ds}}\tau_{\text{data}} + N_{\text{rs}}\tau_{\text{rqt}} \tag{17}$$

TABLE 3. Simulation parameters.

Attribute	Value
Transmission Range	6×6 km
Number of Nodes	20, 50 or 100
Bandwidth	30 kHz
Data Rate	9600bps
Packet Size = Data Slot Size	64, 256, 512 bit
Data Slot Duration (τ_{data})	6.66, 26.66, 53.33 ms
Request Slot Size	8 bit
Request Slot Duration (τ_{rqt})	0.833 ms
Number of Data Slots in Frame (N_{ds})	650, 256 and 128
Number of Request Slots in Frame (N_{rs})	30, 40 and 50
Traffic Load Range	0.1 - 1 Erlangs

V. ANALYSIS OF THE RESULTS

To enable the full realization of the effectiveness of CFDAMA-SRR, the scheme has been simulated and investigated in detail. Comparisons with CFDAMA-RR, round robin free assignment, demand assignment and with the analytical model given in Equation (15) are shown in this section. Comparison with the STUMP protocol [8] is also provided in this section. In all the results presented, channel load is measured in Erlangs and represented as a fraction of the transmitted data. The channel is loaded up to its maximum useful data carrying capacity.

A. COMPARATIVE PERFORMANCE OF CFDAMA-SRR

Fig. 6 shows the mean end-to-end delay performance against a variety of channel loads ranging from 0.1 to 1 Erlang and based on both Poisson and Pareto ON/OFF traffic models. The graphs shown in the figure are for CFDAMA-SRR while the other variants of CFDAMA with different request strategies are shown later. The results show that like other CFDAMA variants, the CFDAMA-SRR scheme consistently outperforms its two constituent schemes (free and demand assignment) in both mean end-to-end delay and channel utilization. The reason behind this is the nature of CFDAMA mechanism in general which is more adaptive to the variation in channel conditions; it exploits the advantages of its two underlying schemes based on the instantaneous value of channel load.

At low to medium channel loads, the end-to-end delay performance with both traffic models is similar to the performance of the free assignment scheme, indicating that the DAMA scheme under these conditions is not invoked yet. This is attributable to the fact that the average packet arrival rate is slower than the rate of assigning free slots in a round robin fashion due to the low level of burstiness. Up to approximately 50% of the channel capacity, the mean end-to-end delay is close to its minimum and is greater with Poisson than Pareto ON/OFF traffic models. This behavior is attributable

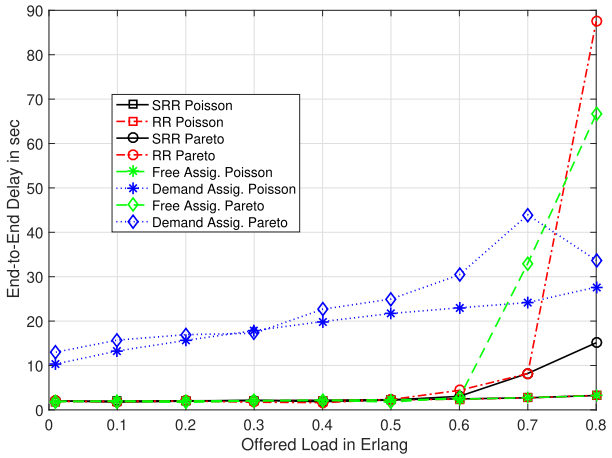

FIGURE 6. Comparative delay/utilization performance of CFDAMA-SRR vs. Round Robin Free assignment vs. Demand assignment with 100 nodes.

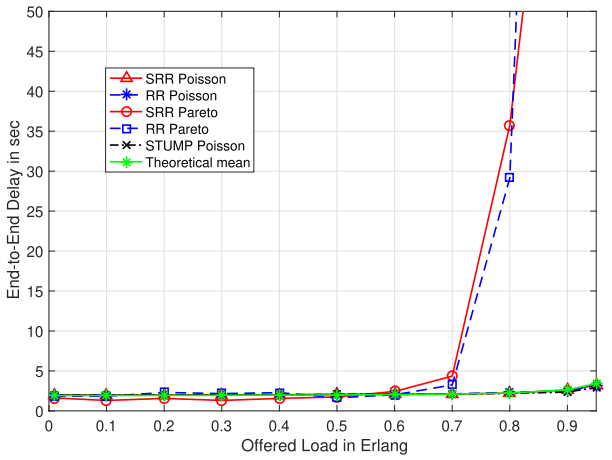

FIGURE 7. Comparative delay/utilization performance of CFDAMA-SRR vs. CFDAMA-RR vs. STUMP with 20 nodes.

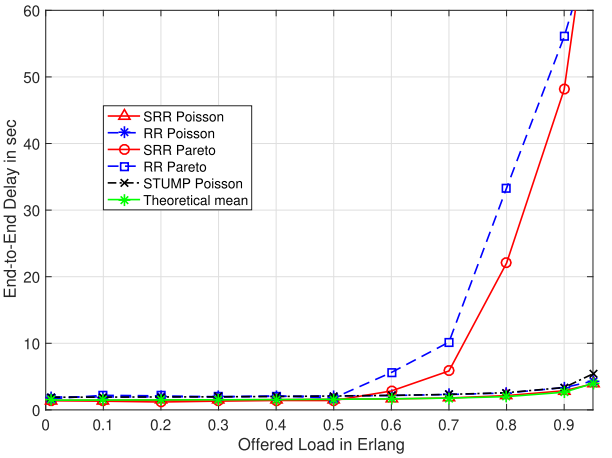

FIGURE 8. Comparative delay/utilization performance of CFDAMA-SRR vs. CFDAMA-RR vs. STUMP with 50 nodes.

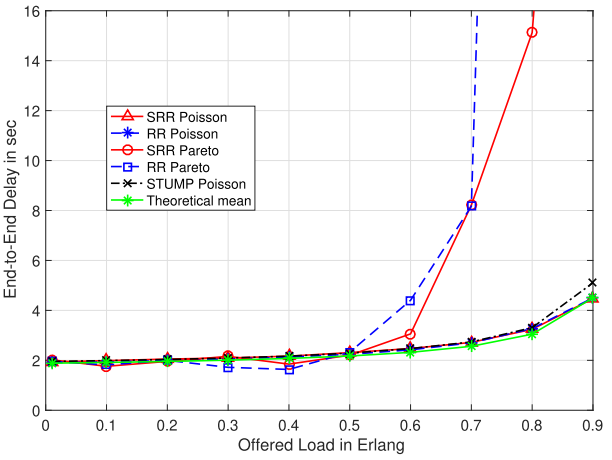

FIGURE 9. Comparative delay/utilization performance of CFDAMA-SRR vs. CFDAMA-RR vs. STUMP with 100 nodes.

to the periodic ON/OFF nature of the traffic source and how often the packet arrivals within bursts are. In this instance, the uniform regularity of low traffic ON/OFF source leads to that every packet could potentially be transmitted in the first free allocated slot just after its arrival. Whereas, in Poisson traffic, the scenario is different where several packets could arrive between successive free slot allocations in some cases. Above 50% of channel capacity, the end-to-end delay is much higher with the Pareto ON-OFF traffic because of the greater burstiness of the ON-OFF data traffic. This is because of the statistics of Pareto ON/OFF data traffic which produce a longer period of time during which the number of nodes generating bursts exceeds a certain sustainable number. If a long burst of packets is generated from a Pareto ON/OFF source, a substantial number of packets would start to build up in the node's queue. This will then result in significant demand by this node and subsequent slot allocation. It means the node will dominate the return frame for a significant period of time. All this will eventually cause a dramatic increase in the mean end-to-end delay at very high channel loads. A key point to note from these results is that despite the significantly longer burstiness of the Pareto ON/OFF traffic compared with traditional Poisson, the CFDAMA-SRR scheme is still capable of providing good end-to-end delay performance up to 90% of channel capacity.

1) SRR vs. RR

The results in Fig. 7, Fig. 8 and Fig. 9 clearly indicate that the CFDAMA-SRR scheme outperforms its underlying scheme CFDAMA-RR in terms of end-to-end delay and channel utilization with the Poisson traffic model and different number of nodes 20, 50 and 100 nodes respectively. CFDAMA-SSR experiences the lowest end-to-end delay throughout almost all channel loads shown in the figures with all simulated network sizes. The minimum end-to-end delay that CFDAMA experiences is at very low traffic load; when the majority of the slots are freely assigned. At high channel loads, the end-to-end delay steadily increases, but the experienced delay rises more slowly with CFDAMA-SRR compared with

CFDAMA-RR. As shown in Fig. 9, at a channel utilization of 1% of the channel capacity and 100 nodes, the minimum end-to-end delay is only 2 s with both traffic models. At a high channel load of 80%, the mean end-to-end delay of CFDAMA-SRR is only 3 s with Poisson and 15 s with Pareto ON/OFF. This enhanced performance of CFDAMA-SRR can be attributable to a number of reasons:

- The scheme has a bias against transmissions associated with long round-trip demand assigned slots. The queuing time is correlated to the node location. Nodes that are located further from the gateway will have more availability of queued packets. Far nodes will also be able to efficiently exploit their request opportunities, and hence, the farther away the node is, the larger number of packets will be served in a request opportunity.
- It allows those nodes which are located closer to the gateway to make their requests first rather than potentially waiting for multiple CFDAMA frames. In the meantime, it allows more time for those nodes which are located further away from the gateway to maximize the use of the available free assigned slots rather than wasting them.
- For the same two reasons above, the likelihood of wasting free assigned slots in some cases due to the potential absence of queued packets at sensor nodes is very low.

2) SRR vs. STUMP

STUMP represents an excellent TDMA-based solution in terms of throughput by transmitting data packets without MAC overhead. It achieves high utilization by exploiting node location diversity to overlap node transmissions and enable ordered packet arrivals. However, its delay/utilization performance dependent on the accuracy of its ordering algorithm. Also, it does not have a mechanism to respond to individual node requirements. Its waiting and service time increases as the value of channel load increases.

Fig. 7, Fig. 8 and Fig. 9 indicate that in virtually all cases both schemes perform similarly. The reason behind this similarity in performance is the limited burstiness of the Poisson traffic that cannot offer substantial demands for an excessive period of time long enough to enable demand assigned slots to contribute effectively. In contrast, free assigned slots in this instance can contribute more effectively to support the transmission of independently generated packets. The overhead of CFDAMA-SRR is negligible in these scenarios owing to long CFDAMA frames. With moderate channel loads, all data slots in the CFDAMA return frame are freely assigned, and hence, the resulting delay/utilization performance is independent of the request strategy. At high offered load values and 100 nodes, CFDAMA-SRR has a small advantage over STUMP in terms of end-to-end delay. This is attributable to the increased demand made for packets having exponential inter-arrival time, and the fact that the TDMA slots assigned periodically by STUMP cannot be as effective as the on-demand slots assigned by CFDAMA-SRR at such high load levels. At a high channel load of 90%, the mean end-to-end delays are around 4.5 s with CFDAMA-SRR, and 5.1 s with STUMP.

B. PERFORMANCE OF CFDAMA-SRR WITH DIFFERENT PARAMETERS

1) REQUEST STRATEGY

Fig. 10 illustrates the delay/utilization performance of CFDAMA with Poisson modeled traffic and different request strategies. It can be seen that choice of request strategy has a small effect on the performance over some parts of the offered load range, becoming clearer at high channel loads with Pareto ON/OFF traffic whose results are shown in the opposite figure - Fig. 11. Considering the results in Fig. 11 obtained with Pareto ON-OFF traffic source, it can be seen that the SRR strategy exhibits superior delay/utilization performance at high channel loads to its substructure - the RR strategy. This is primarily attributable to the fact that CFDAMA-SRR limits the chances of wasting free assigned slots and also biases against demand assigned slots associated with long round-trip delays.

Moreover in Fig. 11, at high channel loads, the end-to-end delay rises rapidly and CFDAMA with both request strategies becomes less effective under Pareto ON/OFF model when the channel is loaded beyond 80% of its capacity. Despite the long burstiness and high channel load, the CFDAMA-SRR scheme is still able to provide acceptable utilization performance up to 85% of channel capacity. Results in both figures (Fig. 10 and Fig. 11) also show that other request strategies (PA and CR) are also outperformed by SRR with Pareto ON/OFF model. In the PA strategy, a small number of nodes hog the channel, which inhibits other nodes from making strongly needed requests. The CR strategy overcomes this issue by combining PA with the RA strategy but still cannot outperform SRR. The CFDAMA-SRR scheme with Pareto ON/OFF traffic has a mean end-to-end delay of around 14 s at channel load of 80% whereas it is above 40 s with the RR scheme.

Considering different numbers of request slots for the CFDAMA-SRR schemes, Fig. 12 and Fig. 13 show the delay/utilization performance with both Poisson and Pareto ON/OFF respectively. It can be seen that changing the number of request slots has almost no noticeable impact on the delay performance at low and medium channel loads with either traffic model.

2) NUMBER OF REQUEST SLOTS

Over the first half of the load range, CFDAMA-SRR relies mainly on the free assignment strategy where request slots are not necessarily required. At high channel loads of Pareto ON/OFF traffic up to 80% of channel capacity, the performance shows a much more sensitive response to the changes in the number of request slots. This is because the increasing number of request slots results in a rise in the frame over-

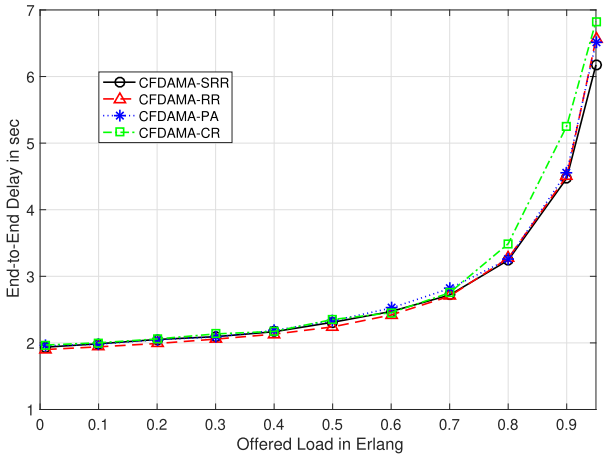

FIGURE 10. CFDAMA-SRR with different request strategies and Poisson traffic condition.

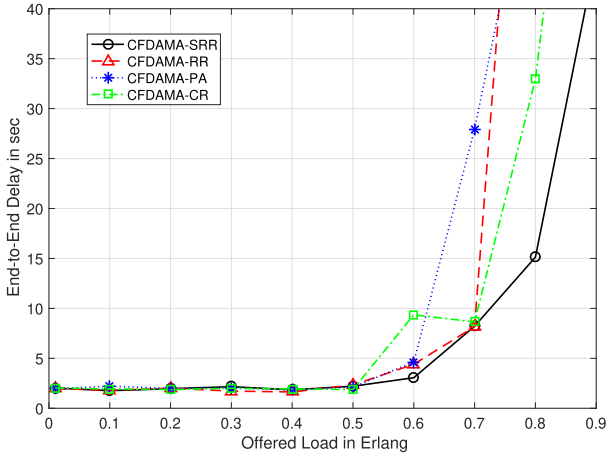

FIGURE 11. CFDAMA-SRR with different request strategies and Pareto ON/OFF condition.

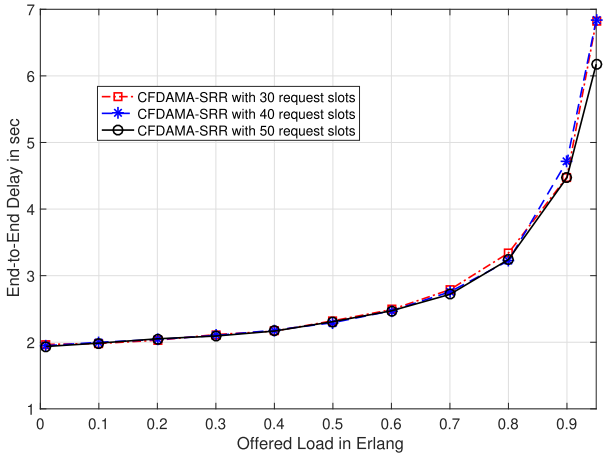

FIGURE 12. CFDAMA-SRR with different number of request slots and Poisson traffic condition.

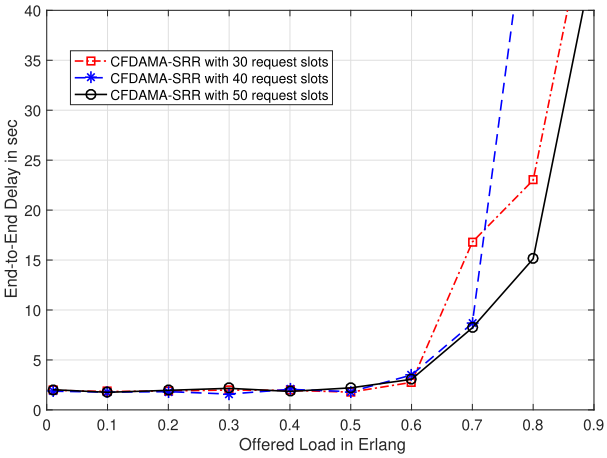

FIGURE 13. CFDAMA-SRR with different number of request slots and Pareto ON/OFF condition.

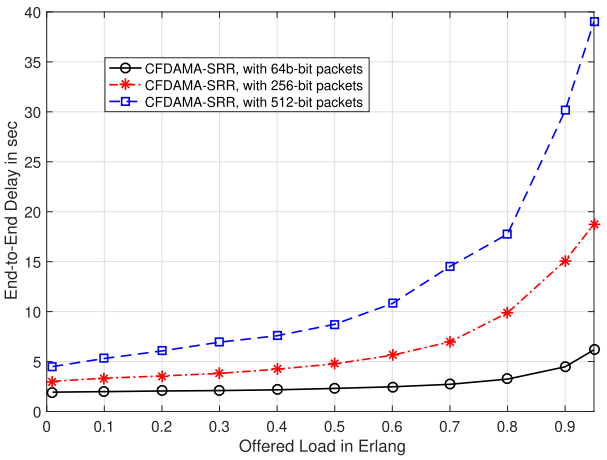

FIGURE 14. CFDAMA-SRR with different packet lengths and Poisson traffic condition.

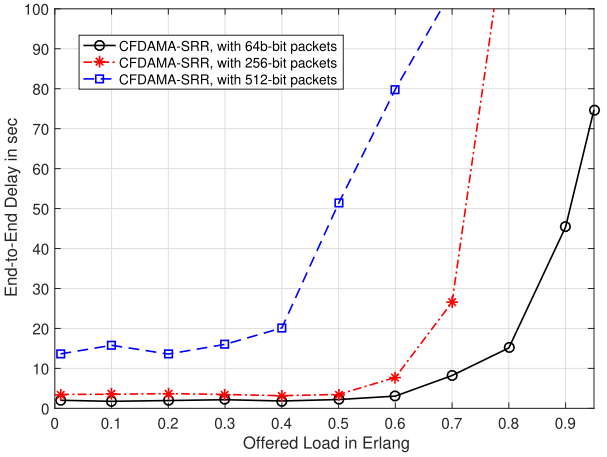

FIGURE 15. CFDAMA-SRR with different packet lengths and Pareto ON/OFF condition.

head and a growth in wasted capacity due to unused request slots. However, a small number of request slots cannot cope with the increasing channel demand causing an increase in the delay of making requests and obtaining assigned slots. With 50 request slots, the mean end-to-end delay is around 8 s at a load of 70% of channel capacity. At high channel

loads, decreasing the number of request slots to 40 slots and then 30 slots resulted in longer delays and inferior channel utilization at high channel loads with Pareto ON/OFF traffic.

3) DATA PACKET SIZE

The impact of different packet sizes on the CFDAMA-SRR performance is shown in Fig. 14 and Fig. 15 with Poisson and Pareto ON/OFF traffic models respectively. The scheme performs better with short packets. This is attributable to the low data rate used, which is the typical date rate of underwater models. Long packets demand long slots in a CFDAMA frame, and long slots can make it less regular for slots to be freely assigned as the free slots are assigned using a round robin method. This increases the average end-to-end delay for long packets transmission. The resulting delay/utilization characteristics with Pareto ON-OFF traffic are more sensitive to the packet size than the characteristics resulted with Poisson traffic model. These results put further emphasis on the notion that it is the periodic ON-OFF nature of the self-similar traffic model that is behind most of the performance differential to Poisson traffic. Unlike with Poisson traffic source, the CFDAMA-SRR delay performance with Pareto ON-OFF traffic source and 1024-bit packets experienced a degradation. This is due to the heavy tail of the Pareto distribution with a high probability of long ON or OFF periods when such long packets are used.

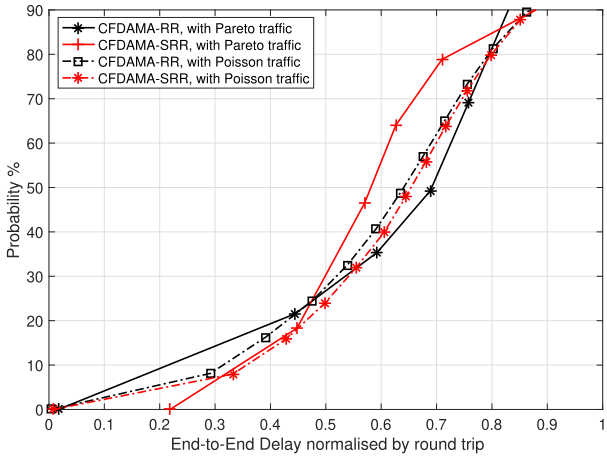

FIGURE 16. Cumulative Distribution Function at 30% offered load, 650 of 64-bit data slots and 50 of 8-bit request slots per frame.

C. END-TO-END DELAY DISTRIBUTION

Fig. 16 and Fig. 17 show the Cumulative Distribution Function of the end-to-end delay (normalized by the average length of round trips) of all packet transmissions for the two strategies (SRR and RR) with 100 nodes and the two traffic types (Poisson and Pareto ON/OFF) at both 30% and 60% load values. For the same reasons explained above, the superiority of SRR is particularly manifested at high channel loads with Pareto ON-OFF traffic. At the 30% offered load value, 90% of packets with both traffic models do not exceed the

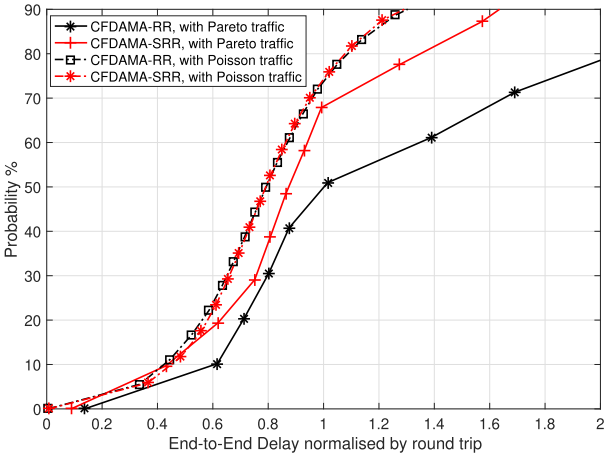

FIGURE 17. Cumulative Distribution Function at 60% offered load, 650 of 64-bit data slots and 50 of 8-bit request slots per frame.

boundary of a round trip. This indicates all the packets are transmitted via free assigned slots. At the 60% offered load value, 35% of RR packets with Pareto ON/OFF experience longer delays than a round trip, whereas 85% of SRR packets do not exceed the boundary of a round trip. With Poisson traffic, both strategies perform similarly and allow 90% of packets to arrive at the destination within a round-trip time.

VI. CONCLUSION

This paper has shown that the CFDAMA protocol offers excellent performance in dealing with the trade-off between end-to-end packet delays and channel utilization with both Poisson and Pareto ON/OFF data traffic types through simulated underwater scenarios. The major advantage of the CFDAMA protocol is the fact that it exploits the contentionless nature of free assignment and the effectiveness of demand assignment in achieving high channel utilization efficiency. At low channel loads, the free assignment strategy provides end-to-end delays closer to the minimum bound of a 0.5 gateway hop. At high channel loads, the free assignment strategy becomes less effective, whereas the demand assignment strategy starts to dominate CFDAMA operations supporting higher channel utilization. A new CFDAMA variant, namely CFDAMA-SRR, more suitable for the underwater environment has been proposed. It incorporates round robin request strategy but in a systematic way, to draw on the advantages of CFDAMA-RR. Simulation results show that CFDAMA-SRR is able to provide superior delay/utilization performance than any other request strategy, with consistent throughput and stable end-to-end delay performance for a wide range of scenarios. With data rates up to 10 kbit/s and with 20, 50 and 100 nodes over a large coverage area, CFDAMA-SRR makes it possible to load the channel up to very high levels of its capacity with a delay performance less than that achievable with CFDAMA-RR. At a high channel load of 80%, the mean end-to-end delay of CFDAMA-SRR is less than 3 s with Poisson and 15 s with Pareto ON/OFF.

REFERENCES

[1] E. Felemban, F. K. Shaikh, U. M. Qureshi, A. A. Sheikh, and S. B. Qaisar, "Underwater sensor network applications: A comprehensive survey," *Int. J. Distrib. Sensor Netw.*, vol. 11, no. 11, 2015, Art. no. 896832.
[2] W. M. Gorma and P. D. Mitchell, "Performance of the combined free/demand assignment multiple access protocol via underwater networks," in *Proc. Int. Conf. Underwater Netw. Syst. (WUWNET)*, New York, NY, USA, 2017, pp. 5:1–5:2.
[3] H. S. Dol, P. Casari, T. van der Zwan, and R. Otnes, "Software-defined underwater acoustic modems: Historical review and the nilus approach," *IEEE J. Ocean. Eng.*, vol. 42, no. 3, pp. 722–737, Jul. 2017.
[4] I. F. Akyildiz, D. Pompili, and T. Melodia, "Underwater acoustic sensor networks: Research challenges," *Ad Hoc Netw.*, vol. 3, no. 3, pp. 257–279, Mar. 2005.
[5] J. Heidemann, M. Stojanovic, and M. Zorzi, "Underwater sensor networks: Applications, advances and challenges," *Philos. Trans. Roy. Soc. London A, Math. Phys. Sci.*, vol. 370, no. 1958, pp. 158–175, Jan. 2012.
[6] E. M. Sozer, M. Stojanovic, and J. G. Proakis, "Underwater acoustic networks," *IEEE J. Ocean. Eng.*, vol. 25, no. 1, pp. 72–83, Jan. 2000.
[7] N. Morozs, P. Mitchell, and Y. V. Zakharov, "TDA-MAC: TDMA without clock synchronization in underwater acoustic networks," *IEEE Access*, vol. 6, pp. 1091–1108, 2018.
[8] K. Kredo, II, P. Djukic, and P. Mohapatra, "Stump: Exploiting position diversity in the staggered TDMA underwater MAC protocol," in *Proc. INFOCOM*, 2009, pp. 2961–2965.
[9] T. Le-Ngoc and J. I. Mohammed, "Combined free/demand assignment multiple access (CFDAMA) protocols for packet satellite communications," in *Proc. 2nd IEEE Int. Conf. Universal Pers. Commun.*, vol. 2, Oct. 1993, pp. 824–828.
[10] A. A. Syed, W. Ye, and J. Heidemann, "Comparison and evaluation of the T-Lohi MAC for underwater acoustic sensor networks," *IEEE J. Sel. Areas Commun.*, vol. 26, no. 9, pp. 1731–1743, Dec. 2008.
[11] W.-H. Liao and C.-C. Huang, "SF-MAC: A spatially fair MAC protocol for underwater acoustic sensor networks," *IEEE Sensors J.*, vol. 12, no. 6, pp. 1686–1694, Jun. 2012.
[12] C. Li, Y. Xu, C. Xu, Z. An, B. Diao, and X. Li, "DTMAC: A delay tolerant MAC protocol for underwater wireless sensor networks," *IEEE Sensors J.*, vol. 16, no. 11, pp. 4137–4146, Jun. 2016.
[13] Q. Wang, "Traffic analysis & modeling in wireless sensor networks and their applications on network optimization and anomaly detection," *Netw. Protocols Algorithms*, vol. 2, no. 1, pp. 74–92, 2010.
[14] W. Gorma, P. Mitchell, and Y. Zakharov, "CFDAMA-IS: MAC protocol for underwater acoustic sensor networks," in *Proc. Int. Conf. Broadband Commun., Netw. Syst.* Cham, Switzerland: Springer, 2018, pp. 191–200.
[15] M. B. Porter, "The bellhop manual and user's guide: Preliminary draft," Heat, Light, Sound Res., San Diego, CA, USA, Tech. Rep. HLS-2010–1, 2011.
[16] P. D. Mitchell, D. Grace, and T. C. Tozer, "Performance of the combined free/demand assignment multiple access protocol with combined request strategies via satellite," in *Proc. 12th IEEE Int. Symp. Pers., Indoor Mobile Radio Commun.*, vol. 2, 2001, pp. 90–94.
[17] P. D. Mitchell, T. C. Tozer, and D. Grace, "Improved medium access control for data traffic via satellite using the CFDAMA protocol," in *Proc. IET Conf.*, Jan. 2000, p. 18.
[18] P. D. Mitchell, D. Grace, and T. C. Tozer, "Comparative performance of the CFDAMA protocol via satellite with various terminal request strategies," in *Proc. IEEE Global Telecommun. Conf. (GLOBECOM)*, vol. 4, Nov. 2001, pp. 2720–2724.
[19] T. LE-NGOC and S. V. Krishnamurthy, "Performance of combined free/demand assignment multiple-access schemes in satellite communications," *Int. J. Satell. Commun.*, vol. 14, no. 1, pp. 11–21, 1996.
[20] W. C. Chan, T.-C. Lu, and R.-J. Chen, "Pollaczek-Khinchin formula for the M/G/1 queue in discrete time with vacations," *IEE Proc.-Comput. Digit. Techn.*, vol. 144, no. 4, pp. 222–226, 1997.
[21] T. S. Rappaport *et al.*, *Wireless Communications: Principles and Practice*, vol. 2. Upper Saddle River, NJ, USA: Prentice-Hall, 1996.
[22] I. S. Hammoodi, B. G. Stewart, A. Kocian, and S. G. McMeekin, "A comprehensive performance study of OPNET modeler for ZigBee wireless sensor networks," in *Proc. Int. Conf. Next Gener. Mobile Appl., Services Technol.*, 2009, pp. 357–362.
[23] W. D. Wilson, "Speed of sound in sea water as a function of temperature, pressure, and salinity," *J. Acoust. Soc. Amer.*, vol. 32, no. 6, pp. 641–644, 1960.
[24] B. Dushaw. (2009). *Worldwide Sound Speed, Temperature, Salinity, and Buoyancy from the NOAA World Ocean Atlas*. [Online]. Available: http://staff.washington.edu/dushaw/WOA/
[25] M. Porter. (Sep. 2017). *Acoustics Toolbox*. [Online]. Available: http://oalib.hlsresearch.com/Modes/AcousticsToolbox/
[26] M. Stojanovic, "On the relationship between capacity and distance in an underwater acoustic communication channel," *ACM SIGMOBILE Mobile Comput. Commun. Rev.*, vol. 11, no. 4, pp. 34–43, 2007.
[27] W. H. Thorp, "Deep-ocean sound attenuation in the sub- and low-kilocycle-per-second region," *J. Acoust. Soc. Amer.*, vol. 38, no. 4, pp. 648–654, 1965.
[28] V. Paxson and S. Floyd, "Wide area traffic: The failure of Poisson modeling," *IEEE/ACM Trans. Netw.*, vol. 3, no. 3, pp. 226–244, Jun. 1995.
[29] W. E. Leland, M. S. Taqqu, W. Willinger, and D. V. Wilson, "On the self-similar nature of Ethernet traffic (extended version)," *IEEE/ACM Trans. Netw.*, vol. 2, no. 1, pp. 1–15, Feb. 1994.
[30] A. Mainwaring, D. Culler, J. Polastre, R. Szewczyk, and J. Anderson, "Wireless sensor networks for habitat monitoring," in *Proc. 1st ACM Int. Workshop Wireless Sensor Netw. Appl.*, 2002, pp. 88–97.
[31] A. K. Mohapatra, N. Gautam, and R. L. Gibson, "Combined routing and node replacement in energy-efficient underwater sensor networks for seismic monitoring," *IEEE J. Ocean. Eng.*, vol. 38, no. 1, pp. 80–90, Jan. 2013.
[32] C. Petrioli, R. Petroccia, J. Shusta, and L. Freitag, "From underwater simulation to at-sea testing using the ns-2 network simulator," in *Proc. IEEE OCEANS*, Jun. 2011, pp. 1–9.

WAEL GORMA received the B.Sc. degree in electrical engineering from the University of Misurata, in 2008, and the M.Sc. degree in electronic engineering from both the Nottingham Trent University and the College of Industrial Technology (CIT), in 2012. He has held lecturing positions for two years at CIT and others. He is currently pursuing the Ph.D. degree in medium access control for underwater acoustic sensor networks with the Communication Technologies Research Group, Electronic Engineering Department, University of York. His research interests include multiple-access and medium-access control and sharing for wireless radio, and acoustic sensor networks in extreme environments.

PAUL D. MITCHELL (M'00–SM'09) received the M.Eng. and Ph.D. degrees from the University of York, in 1999 and 2003, respectively. His Ph.D. research was on medium-access control for satellite systems, which was supported by British Telecom. He has been a member of the Department of Electronic Engineering, University of York, since 2002, and is currently a Reader. He has gained industrial experience at BT and QinetiQ. He has authored over 110 refereed journals and conference papers and has served on numerous international conference program committees. His current research interests include medium-access control and networking for underwater and mobile communication systems, and the application of artificial intelligence techniques to such problems. He is currently a Lead Investigator of EPSRC USMART (EP/P017975/1) and a Co-Investigator of H2020 MCSA 5G-AURA. He was the General Chair of the International Symposium on Wireless Communications Systems which was held in York, in 2010, and the Track Chair of IEEE VTC, in 2015. He is an Associate Editor of the *IET Wireless Sensor Systems* journal and the *Sage International Journal*.

NILS MOROZS (S'13–M'17) received the M.Eng. and Ph.D. degrees in electronic engineering from the University of York, in 2012 and 2015, respectively. His Ph.D. research was part of the EU FP7 ABSOLUTE Project where he developed LTE-compliant dynamic spectrum access methods for disaster relief and temporary event networks. Afterward, he was a Researcher in Wi-Fi and wireless convergence at BT, Martlesham, U.K., and a Research Associate in HAP-based communications with the Department of Electronic Engineering (EE), University of York, where he is currently a Research Associate involved in channel modeling and medium-access control for underwater acoustic sensor networks as part of the EPSRC USMART project (EP/P017975/1). His research interests include the development of protocols, and architectures for wireless radio and acoustic networks.

YURIY V. ZAKHAROV received the M.Sc. and Ph.D. degrees in electrical engineering from the Power Engineering Institute, Moscow, Russia, in 1977 and 1983, respectively. From 1977 to 1983, he was with the Special Design Agency in the Moscow Power Engineering Institute. From 1983 to 1999, he was with the N. N. Andreev Acoustics Institute, Moscow. From 1994 to 1999, he was with Nortel as a DSP Group Leader. Since 1999, he has been with the Communications Research Group, University of York, U.K., where he is currently a Reader with the Department of Electronic Engineering. His research interests include signal processing, communications, and acoustics.